ALLAN R. JABLON, CRAIG R. MOORE, and JOHN E. PENN

MICROWAVE COMPONENT ANALYSIS USING A NUMERICAL ELECTROMAGNETIC FIELD SOLVER

With the recent development of numerical electromagnetic field solvers, microwave engineers can accurately predict the performance of arbitrarily shaped electromagnetic structures. This article describes the use of a numerical electromagnetic field solver in the analysis of specific microwave components including transitions, waveguide structures, monolithic microwave integrated circuits, and microstrip antennas. Multipactor breakdown analysis is also discussed.

INTRODUCTION

Accurate modeling and analysis of microwave circuit components are essential for the efficient, cost-effective design of microwave systems. In the past, modeling of microwave components consisted of empirical, static, and quasi-static models, many of which lacked sufficient accuracy. Many waveguide components and transitions were too complex to model, and only costly cut-and-try techniques could be used in their design.

With the advent of numerical electromagnetic field solvers, three-dimensional microwave structures can be accurately modeled. Numerical electromagnetic field solvers save time and money because of fewer design iterations. Microwave components that are now accurately modeled include monolithic microwave integrated circuit (MMIC) components, waveguide components, transitions between transmission media, and certain antenna problems. Since numerical electromagnetic field solvers generate electric field data, system problems, such as multipactor breakdown analyses, can also be solved. Microwave engineers in the APL Space Department have used a numerical electromagnetic field solver to analyze microwave components and problems. This article discusses some of the analyses and problem solutions.

THE HIGH-FREQUENCY STRUCTURE SIMULATOR

We used the Hewlett-Packard high-frequency structure simulator (HFSS)[1] as the primary numerical electromagnetic field solver. The HFSS is a finite-element-based software package that solves Maxwell's equations in microwave structures. The region inside an arbitrarily shaped structure, such as a waveguide-to-coaxial transition, is broken into a mesh of tetrahedra (Fig. 1). The electric and magnetic fields inside each tetrahedron are approximated with a polynomial function containing unknown amplitudinal coefficients. The solution is obtained by computing these coefficients. The mesh is refined iteratively until the errors are reduced to an acceptable level, producing a converged solution. Since the solution process generates large matrices of electromagnetic field data and
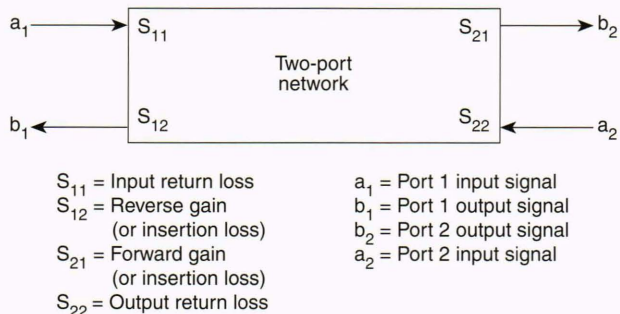
is memory- and processor-intensive, a very fast computer with a large hard disk and with a large random access memory (RAM) is needed to solve problems. A typical configuration includes a 57-million-instructions-per-second (MIPS) processor with 64 Mbytes of RAM and a 750-Mbyte hard disk.

The primary output of the HFSS analysis is the scattering (S) parameters for the component under analysis. S-parameters describe the relationship between the input, output, and reflected signals of a component or circuit (Fig. 2). In addition to the S-parameter output, the HFSS can display graphical representations of electric and magnetic fields. These fields can also be viewed moving
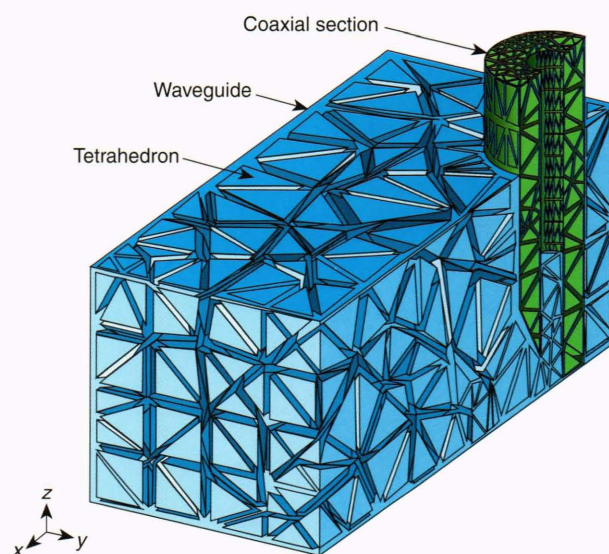
Figure 1. To solve Maxwell's equations in a microwave structure, the region inside the structure, such as this waveguide-to-coaxial transition, is broken into a mesh of tetrahedra. The electric and magnetic fields inside each tetrahedron are then approximated with a polynomial function containing unknown amplitude coefficients. The solution is obtained by computing these coefficients.

S_{11} = Input return loss
S_{12} = Reverse gain
    (or insertion loss)
S_{21} = Forward gain
    (or insertion loss)
S_{22} = Output return loss

a_1 = Port 1 input signal
b_1 = Port 1 output signal
b_2 = Port 2 output signal
a_2 = Port 2 input signal

Figure 2. Scattering parameters are voltage ratios between the signals entering a circuit and the signals exiting the circuit. The nomenclature S_{nm} signifies the ratio of a signal exiting port n (i.e., connection point) to an input signal applied at port m. For example, an amplifier with port 1 as its input and port 2 as its output is described by its forward gain as S_{21}, its reverse gain as S_{12}, and its input and output return losses as S_{11} and S_{22}, respectively. A symmetric, lossless, two-port passive structure, unlike an amplifier, passes signals equally in both directions ($S_{21} = S_{12}$), and the input and output impedances (or return losses) are equal ($S_{11} = S_{22}$). For passive structures, S_{21} and S_{12} are also known as "insertion losses."

through the structure as a function of time. This capability gives the microwave engineer valuable insight into the operation of microwave structures.
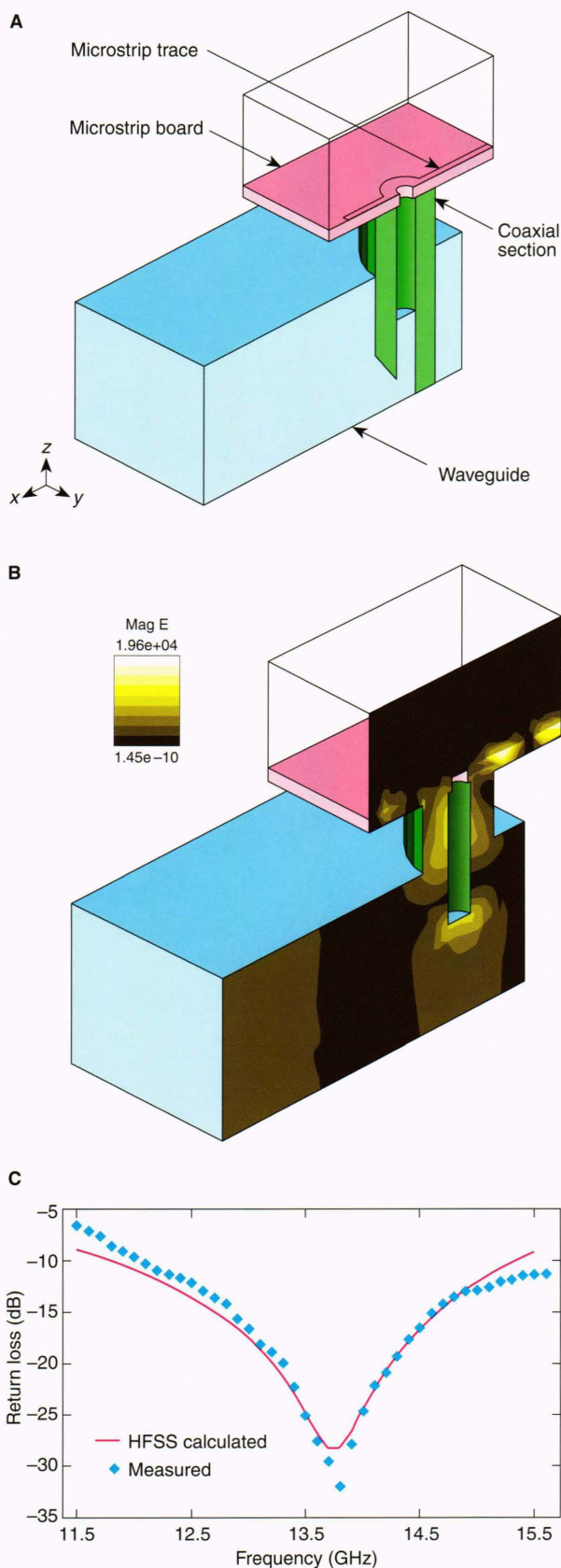
MICROWAVE TRANSITION ANALYSIS

Numerical electromagnetic field solvers are particularly useful for the analysis of mixed media structures such as waveguide-to-microstrip transitions. Several transitions between microwave transmission media have been analyzed, including several waveguide-to-microstrip transitions and a stripline-to-coaxial transition.

Waveguide-to-Microstrip Transitions

Microwave engineers at APL developed a waveguide-to-microstrip transition (Fig. 3) for an array of MMIC transmit–receive modules. The measured and HFSS calculated return losses are shown in Figure 3C. The HFSS calculated data are in close agreement with the measured data, confirming the accuracy of the analytical tool.
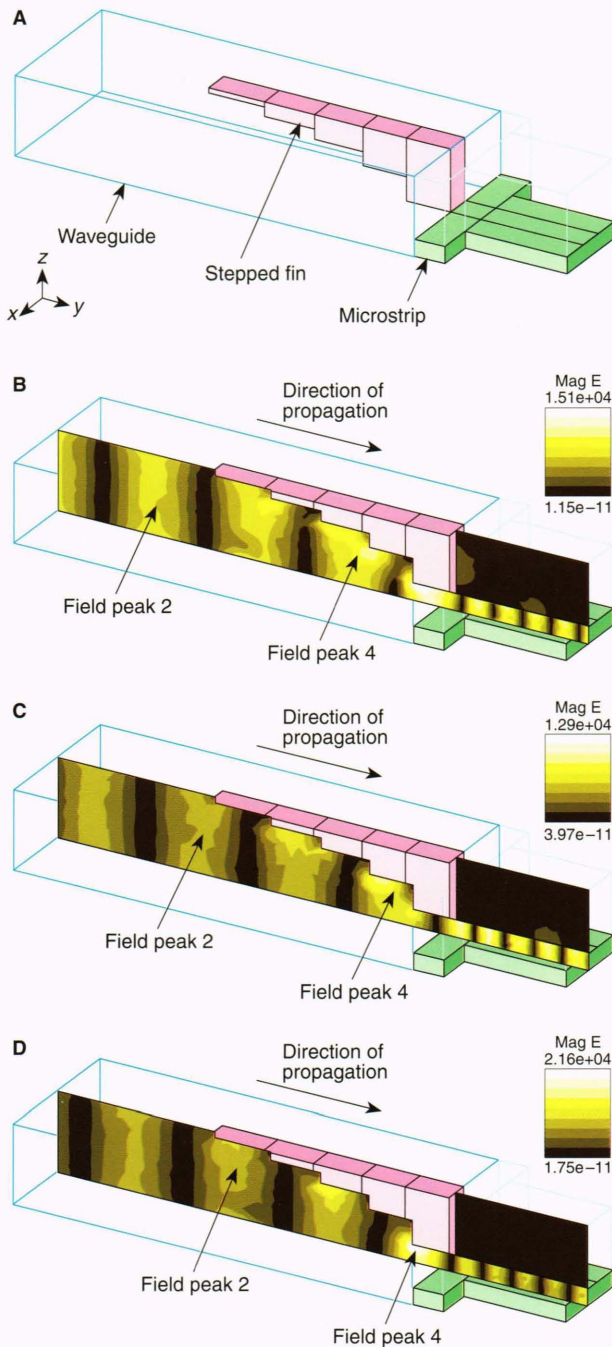
The waveguide-to-microstrip transition was designed using cut-and-try techniques; many iterations were needed to produce the final design, and the process was time-consuming and costly. The use of a numerical electromagnetic field solver would have eliminated the need for the physical design iterations, and the transition could have been built only once, after the design and analysis were complete. The analysis took advantage of the symmetry of the transition (Fig. 3A) to reduce computation time and disk usage. If an object has geometric symmetry, the HFSS field solution can be obtained by solving for the fields in only half the structure. Since the solution matrix is reduced, the use of symmetry saves processor time, RAM, and disk storage space. Figure 3B shows an electric field plot generated by the HFSS.

Numerical electromagnetic field solvers are particularly useful for analysis of mixed media structures such as a 30-GHz stepped fin waveguide-to-microstrip transition (Fig. 4A). The stepped fin structure serves to concentrate

Figure 3. Waveguide-to-microstrip transition analysis. **A.** High-frequency structure simulator (HFSS) model. **B.** Electric field plot generated by HFSS (Mag E: magnitude of electric field [volts/meter]). **C.** Measured and calculated return losses.

Figure 4. Stepped fin waveguide-to-microstrip transition: **A.** High-frequency structure simulator (HFSS) model. **B.** through **D.** Sequence of field plots shows a wave propagating through the transition in phase steps of 60° (Mag E: magnitude of electric field [volts/meter]).

the electric field into a cross section with dimensions comparable to the microstrip structure. The fins were designed using quarter-wavelength transformer theory, which gives ratios of the impedances at each step. The HFSS was used to quickly develop a curve of impedance and wavelength versus single fin depth in WR28 (26.5 to 40 GHz) waveguide. This analysis was performed because the literature deals only with dual (symmetric)

finned waveguide. The HFSS was also used to determine the depth of the final fin for optimum coupling into the 25-mil-thick alumina microstrip. Figures 4B to 4D show the electric field distribution in the vertical central plane as the exciting field is varied in 60° increments. This phase variation has the effect of duplicating the animation available on the workstation screen that shows the energy moving down the waveguide and into the microstrip. The sequence shows that energy attempts to radiate into the transverse electric rectangular waveguide (TE$_{10}$) mode off the back of the final fin. Therefore, it is important to house the microstrip in a waveguide beyond cutoff to prevent energy loss to this unwanted mode. Some work on the dimensions of the step preceding the final fin could improve the reflection coefficient.

Stripline-to-Coaxial Transition

Engineers at APL designed a stripline-to-coaxial transition (Fig. 5) for a microstrip antenna array. The transition includes a guard trace, or mode suppressor, to prevent a parallel-plate waveguide mode from propagating beyond the end of the stripline trace. The guard trace is connected to the top and bottom stripline ground planes using via holes. The top dielectric layer of the stripline is shown in Figure 5A using its tetrahedra mesh. The bottom stripline dielectric layer and the coaxial section are drawn as solids. Once again, the symmetry of the structure was used to reduce computation time.

Figure 5B is a field plot showing the electric field crossing the transition; the figure shows the utility of the HFSS in simulating connections between layers in multilayer microwave boards. Multilayer boards will become increasingly common in the future for phased-array antenna feed networks.

WAVEGUIDE COMPONENT ANALYSIS

Microwave engineers at APL designed a five-port, radial-cavity, E-plane, rectangular waveguide junction at 32 GHz according to a recently published theory.[2] Engineers analyzed the design (Fig. 6A) at several frequencies across the waveguide band. The scattering parameters produced by swept frequency analysis (Fig. 6C) indicated that the equal amplitude power split occurs at 35 GHz instead of the 32-GHz design frequency. Figure 6B shows the HFSS simulation at 35 GHz, where equal-amplitude incident signals of appropriate phase delay on four ports are summed coherently at the fifth port.

A nine-way power splitter in WR62 (12 to 18 GHz) waveguide is shown in Figure 7A; the electric field distribution at 15 GHz in the central plane and at each port is shown in Figure 7B. Nine-way power splitter waveguide problems are analyzed fairly quickly since the aspect ratio between the smallest and largest feature is usually only about 10. Structures that combine waveguide and microstrip often have aspect ratios exceeding several hundred and take hours to solve.

MMIC COMPONENT ANALYSIS

Design engineers can use numerical electromagnetic field solvers to aid in the design of MMIC's. Determining parasitics and coupling between closely spaced compo-
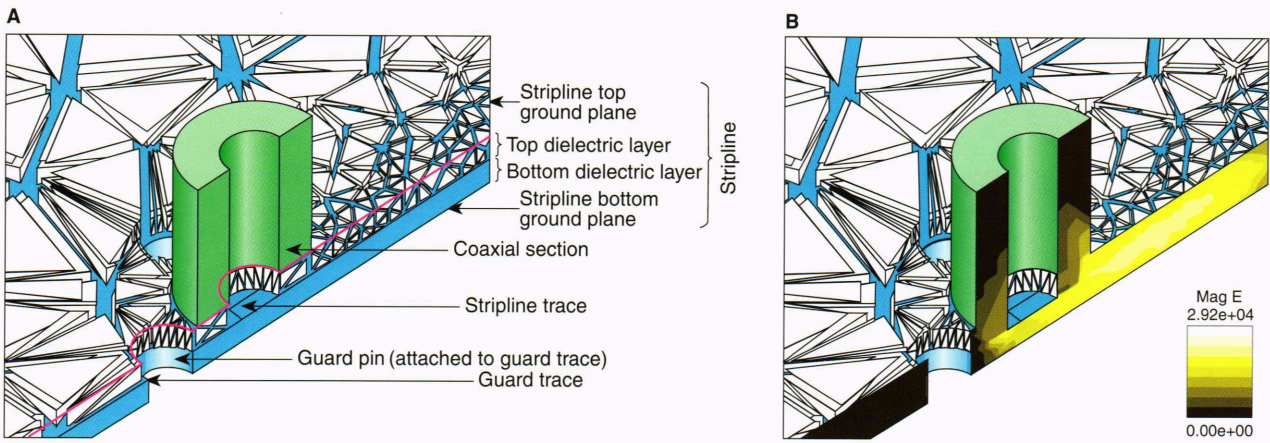
Figure 5. Stripline-to-coaxial transition for a microstrip antenna array. **A.** High-frequency structure simulator (HFSS) model. **B.** Electric field plot (Mag E: magnitude of electric field [volts/meter]).

nents in a MMIC layout is one area where field solvers such as the HFSS are invaluable. A field solver is also invaluable in accurately analyzing transitional structures such as a launch from a coplanar electromagnetic field into a microstrip on the MMIC. Linear simulators are normally used to analyze microwave circuits and MMIC's; but linear simulators, which use empirical and theoretical mathematical models to analyze the circuits, are not capable of determining electromagnetic field effects such as parasitics and coupling between circuit components. Reference 3 compares linear simulator models, measurements, and HFSS simulations done at APL for some MMIC capacitors, inductors, and a few microstrip structures; Reference 3 also reports the close agreement between HFSS simulations and measurements for various MMIC elements. Three examples of MMIC structures that require a field solver are coplanar-to-microstrip launches, MMIC 50-Ω calibration standards, and ganged transistor feed for a power amplifier.
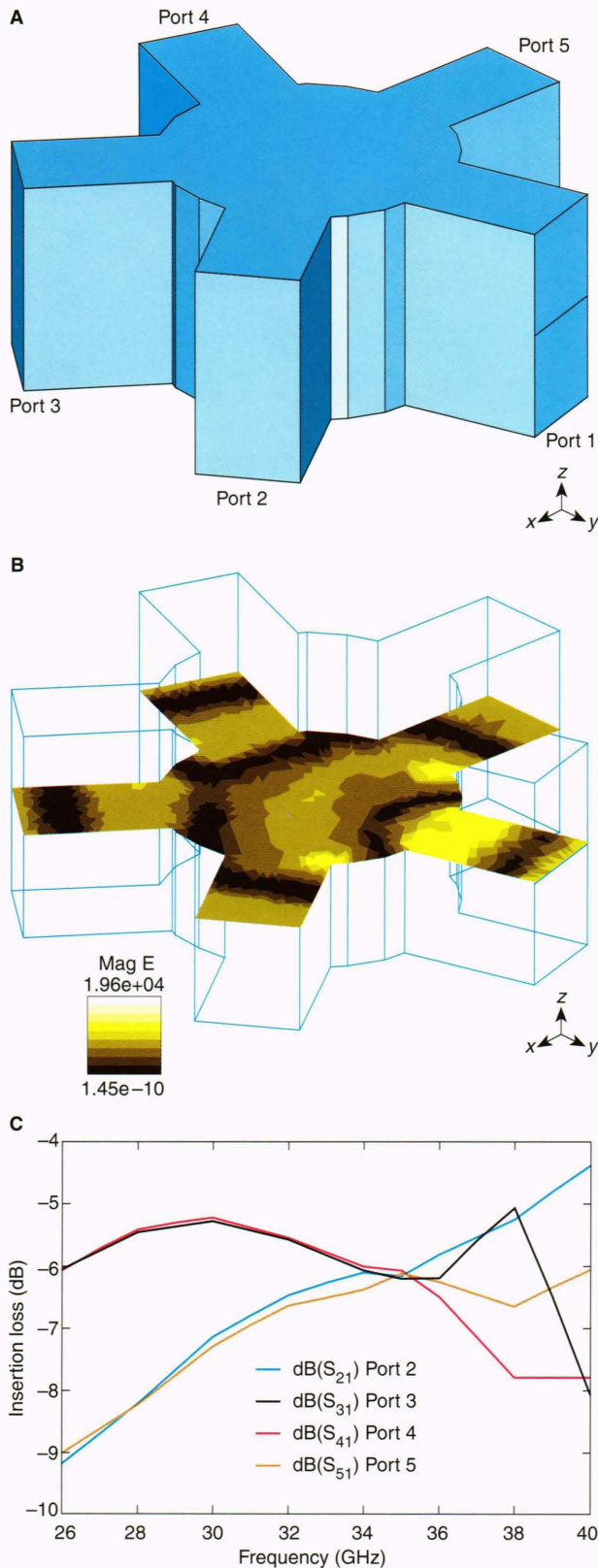
Coplanar-to-Microstrip Launch

Numerical electromagnetic field solvers can be invaluable in the analysis of physical or electrical transitions used in component packaging or in changes in propagation modes. Wafer probe stations employed for MMIC testing use coplanar launches. A MMIC design typically uses a microstrip for interconnection. A MMIC coplanar-to-microstrip launch (Fig. 8A) provides a low-loss, well-matched transition between the probe station and the MMIC under test. Linear simulation of this launch is not sufficiently accurate when the launch is part of an on-wafer calibration standard. A more accurate determination of the coplanar launch characteristics has been made by numerically extracting the S-parameters for a single launch from a measurement of two launches back-to-back (i.e., there is no method for measuring a single launch). The numerical extraction method for deriving S-parameters for two sequential or ganged launches is a good approximation, but it does not have a unique solution for the S_{11} and S_{22} of the launch. Because of the symmetry of the two back-to-back launches, only two unique measurements are obtained for the ganged launch

(i.e., $S_{11}* = S_{22}*$; $S_{12}* = S_{21}*$ [*S-parameters of two back-to-back launches]). However, the single launch is not symmetrical and thus has three unknowns (S_{11}, S_{22}, and $S_{12} = S_{21}$), which are solved by assuming that the input and output impedances are equal ($S_{11} = S_{22}$). (S_{11}-input return loss; S_{12}-reverse gain; S_{21}-forward gain; S_{22}-output return loss).

The launch has been simulated using the HFSS and has been compared with the numerically extracted S-parameters. Figure 8B shows the launch entered into the HFSS with the launch structure formed by a 100-μm-thick gallium arsenide substrate and the metal conductor. Figure 8C shows the electric field lines at the coplanar side of the launch, and Figure 8D shows the electric field lines on the microstrip side. Visualizing the field lines with HFSS gives insight into some of the problems of transitioning propagation modes; visualizing the field lines also shows that the design is operating in the modes desired and that no unanticipated extraneous propagation modes dominate its operation.

In the HFSS simulation, S_{11} and S_{22} are nearly equal in magnitude but not in phase. Since physical differences between the two ends of the launch exist, the results correspond to intuitive expectations. Simulations of loss in the launch are not predicted as well with HFSS as with the numerical extraction. Figure 9 shows the simulation results. A hybrid S-parameter description of the launch using HFSS's predicted input and output impedances and the numerically extracted insertion loss would seem to be a reasonable description of the launch characteristics. Given the accuracy of the measurements, this hybrid launch description could not be proved to be better than the numerically extracted S-parameters. Besides the measurement limitations, another limit was that the HFSS analysis of the launch structure required considerable computing resources. A machine with 57 MIPS, 192 Mbytes of RAM, and over 1 Gbyte of disk space was required to achieve reasonable convergence. Even with the additional solve iterations allowed by a machine with this power, it was still difficult to determine when the HFSS solution was sufficiently converged.
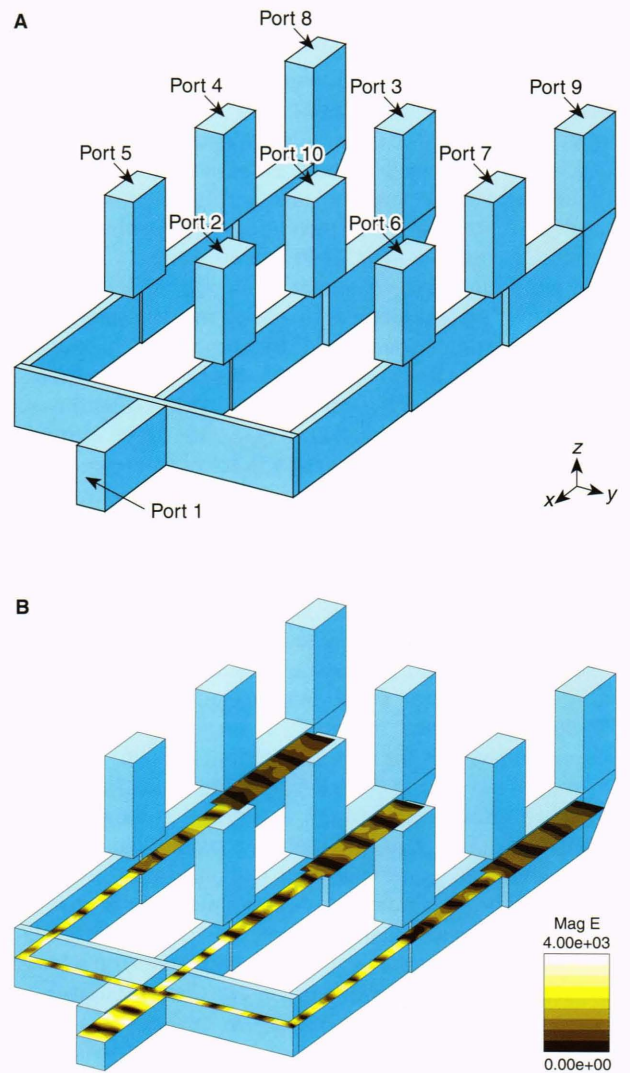
MMIC 50-Ω Calibration Standard

Several recent APL MMIC designs included on-wafer calibration standards, which provided very good measurement agreement with several different calibration techniques up to about 26 GHz. When attempts were made to measure up to 50 GHz, the measurement accuracies and the limited ability to measure the coplanar-to-microstrip launches did not yield the close agreement observed up to 26 GHz.

The HFSS provided insight into why one of the calibration standards could not be accurately used. Two 100-Ω resistors connected in parallel across the coplanar-to-microstrip launch (Fig. 10A) provided a 50-Ω resistance to ground as a measurement standard. An attempt was made to de-embed the launch structure from the resistor measurement using the numerically extracted S-parameters for the launch. By analyzing the electromagnetic

Figure 6. Five-port, radial-cavity, E-plane, rectangular waveguide junction analysis. **A.** High-frequency structure simulator (HFSS) model. **B.** Electric field plot (Mag E: magnitude of electric field [volts/meter]). **C.** Scattering parameters.

Figure 7. Nine-way power splitter in WR62 waveguide. **A.** High-frequency structure simulator (HFSS) model. **B.** Electric field distribution (Mag E: magnitude of electric field [volts/meter]).
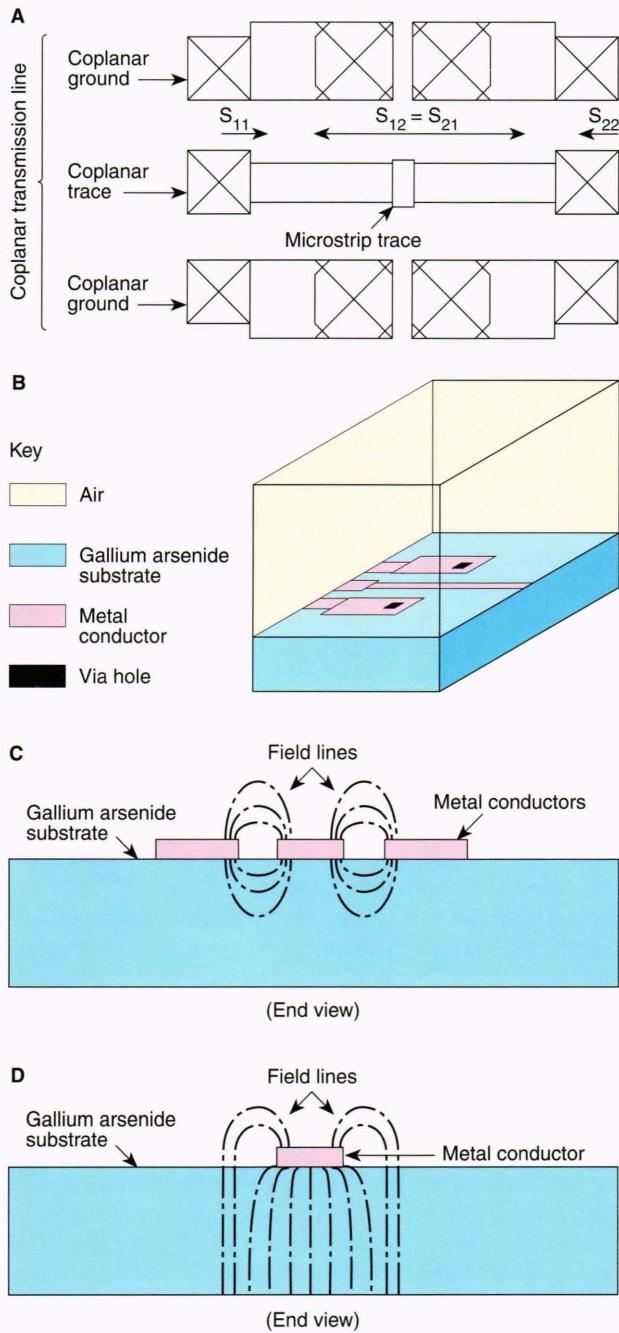
Figure 8. Monolithic microwave integrated circuit (MMIC) coplanar-to-microstrip launch analysis. **A.** Two back-to-back coplanar-to-microstrip launches (short through). **B.** High-frequency structure simulator (HFSS) model. **C.** Coplanar mode electric field (end view). **D.** Microstrip mode electric field (end view).

Simulations of both types of 50-Ω terminations are shown in Figure 10C. The HFSS simulation of the launch connected to two 100-Ω resistors in parallel as a coplanar 50-Ω termination agrees reasonably well with the measured data. In Figure 10C, RAWR50 is the measurement of a launch plus the coplanar termination. The HFSS simu-
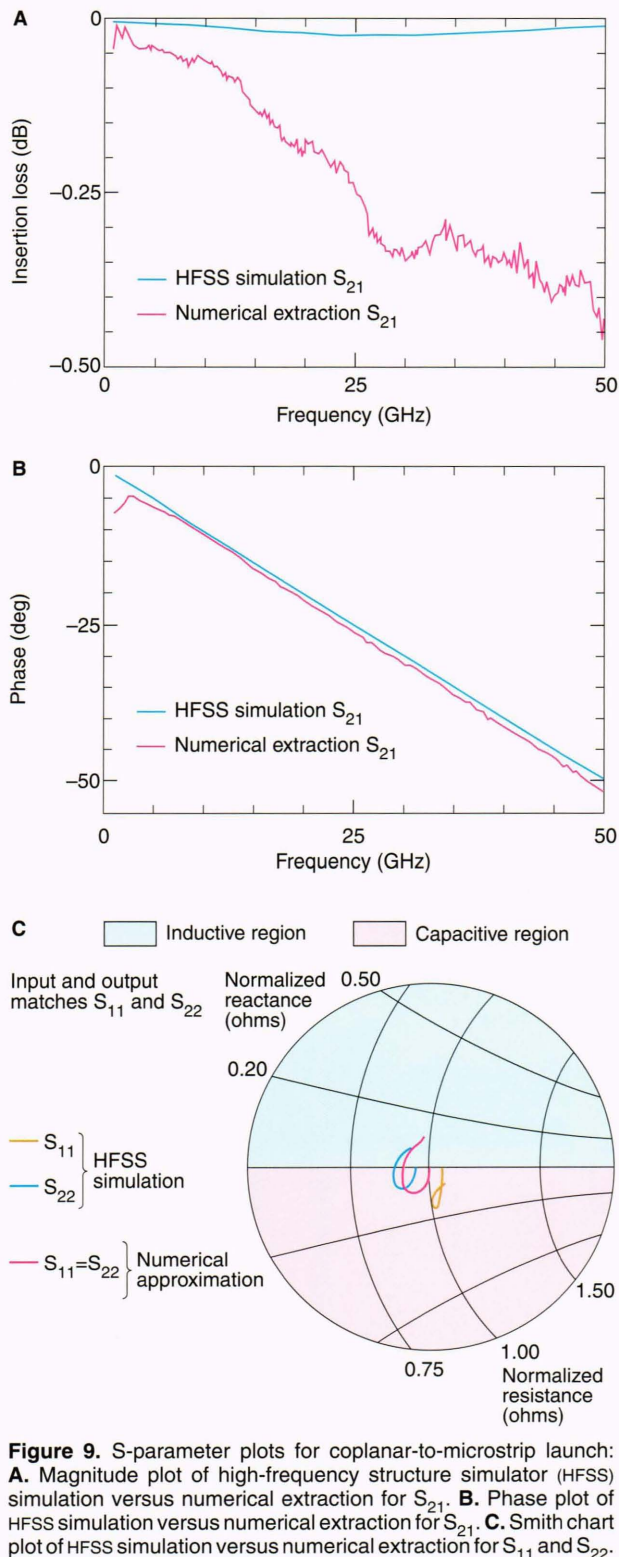
Figure 9. S-parameter plots for coplanar-to-microstrip launch: **A.** Magnitude plot of high-frequency structure simulator (HFSS) simulation versus numerical extraction for S_{21}. **B.** Phase plot of HFSS simulation versus numerical extraction for S_{21}. **C.** Smith chart plot of HFSS simulation versus numerical extraction for S_{11} and S_{22}.

propagation modes, the flaw in the de-embedding technique was realized. Two back-to-back launches were measured where the coplanar mode from the probe station changed to a microstrip mode in the substrate and then back into the coplanar mode. In the calibration standard used, the coplanar mode launched from the probe head never changed to a microstrip mode because the two resistors formed a coplanar termination. The calibration standard must terminate in a 50-Ω impedance that forces the electric field into the microstrip mode (Fig. 10B).

lation COPMCR50 of the coplanar 50-Ω termination matches fairly well. If the resistor terminates in a "microstrip mode," then the results with the launch are dramatically different from the launch with resistors in a coplanar

configuration. In Figure 10C, COPMR502 is the HFSS simulation of a resistor terminated after the microstrip mode is launched.

Ganged Transistor Feed for a Power Amplifier

When designing a power amplifier, several field-effect transistors (FET) are typically combined in the final amplifier stage to increase the power output. For a recent MMIC power amplifier designed at APL, engineers used a simple feed structure to combine four FET's in the final stage of the amplifier. Balancing the electrical lengths of the input and output feeds to the four FET's is critical so that the output power will combine in phase. Any phase imbalance tends to decrease the output power. Figure 11A is a schematic and layout of the linear simulation of the feed structure used in one of the amplifier designs. The feed is nearly symmetrical, but the feeds to the two middle FET's may parasitically couple back to the main feed. The HFSS was used to simulate this structure and compare the phases. As expected, a relatively small phase imbalance occurred for this design (Figs. 11B and 11C). A 6° phase imbalance at 13.6 GHz is negligible, but at a higher frequency this feed design would cause a pronounced loss of power.

MICROSTRIP ANTENNA ANALYSIS

The Laboratory has used a numerical electromagnetic field solver to aid in the design of microstrip antennas. Although antenna analysis is computationally intensive because of the requirement for a boundary approximating free space, analysis using HFSS provides valuable insight into the operation of the microstrip antenna. Any structure analyzed by the HFSS must be completely surrounded by boundaries perfectly conductive by default; these boundaries can also be redefined as ports, perfect magnetic boundaries, imperfectly conducting boundaries, or as resistive surface boundaries.

The simulation of free space is required for accurate antenna simulation. For the microstrip antenna, free space is simulated by creating a hemispherically shaped air dielectric space above the antenna and by defining the boundary between the hemisphere and the background as a 377-Ω-per-square resistive surface. Figure 12A shows the HFSS structure for a coaxial-probe-fed microstrip antenna. The analyzed structure has been cut in half to take advantage of symmetry.

Microwave engineers at APL have successfully modeled two different microstrip antennas and determined their return losses. Modeling can be used to help determine the optimum location for the feed probe, the bandwidth, and the effects of different substrate thicknesses and dielectric constants. Using the HFSS graphical field output option, a propagating wave can be seen (Fig. 12B) traveling from the microstrip patch edges to the 377-Ω resistive boundary for a 10-GHz microstrip antenna. Figure 12B clearly illustrates the radiation of the fields from the microstrip antenna edges. The field display gives the design engineer valuable insight into the operation of the antenna.

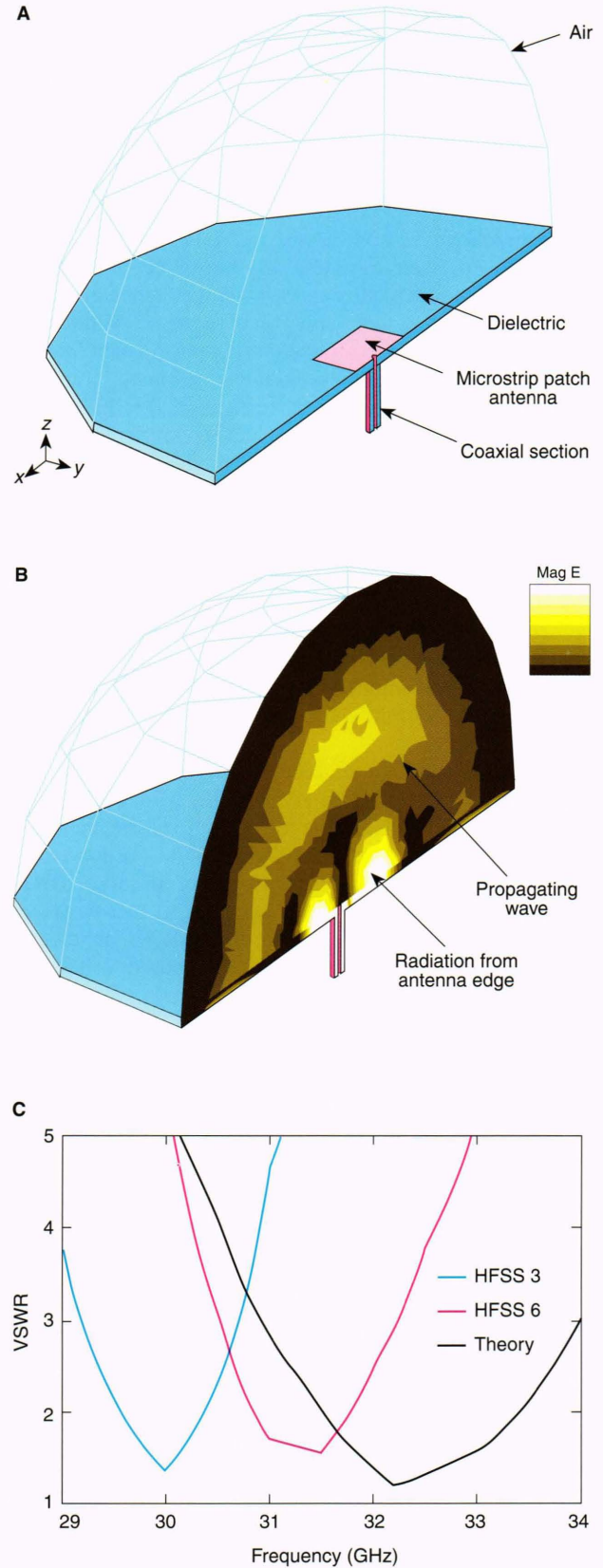Engineers conducted an HFSS simulation for a microstrip patch radiator at 31.5 GHz. The swept-frequency
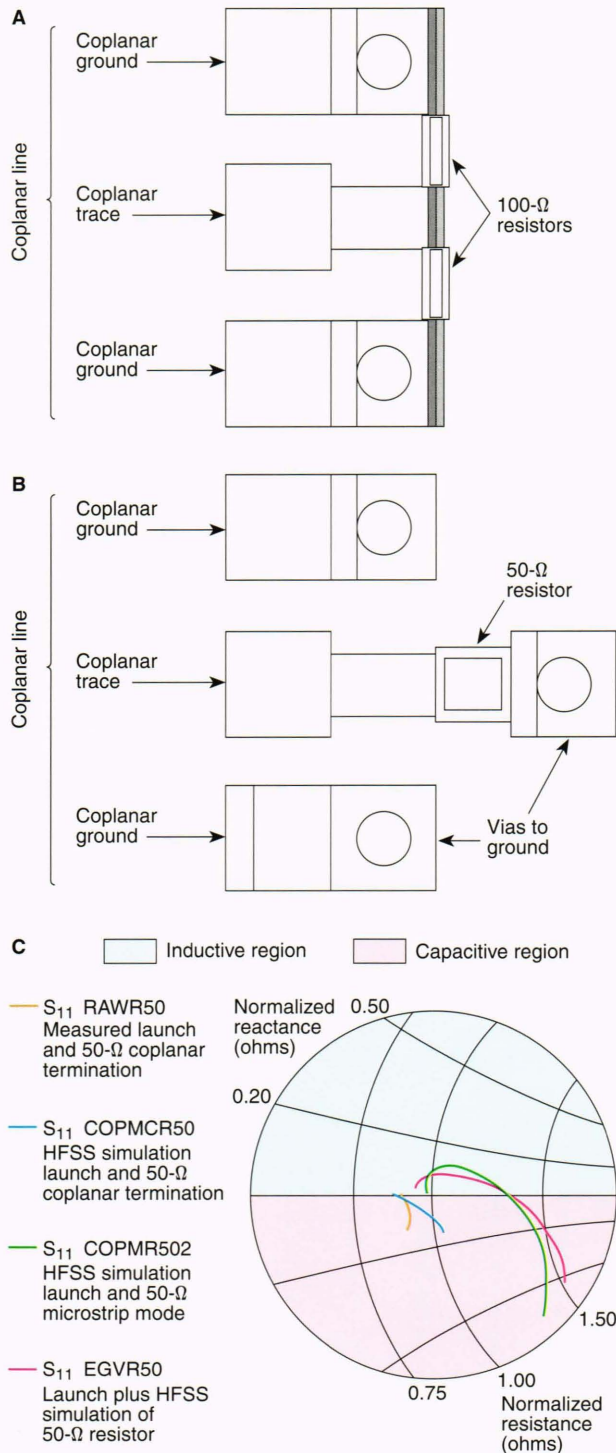
Figure 10. Monolithic microwave integrated circuit 50-Ω calibration standard analysis. **A.** Coplanar-to-microstrip launch with coplanar termination. **B.** Coplanar-to-microstrip launch with series termination. **C.** Differences in coplanar launch with 50-Ω coplanar termination versus 50-Ω microstrip mode termination (HFSS = high-frequency structure simulator).

A

B

C
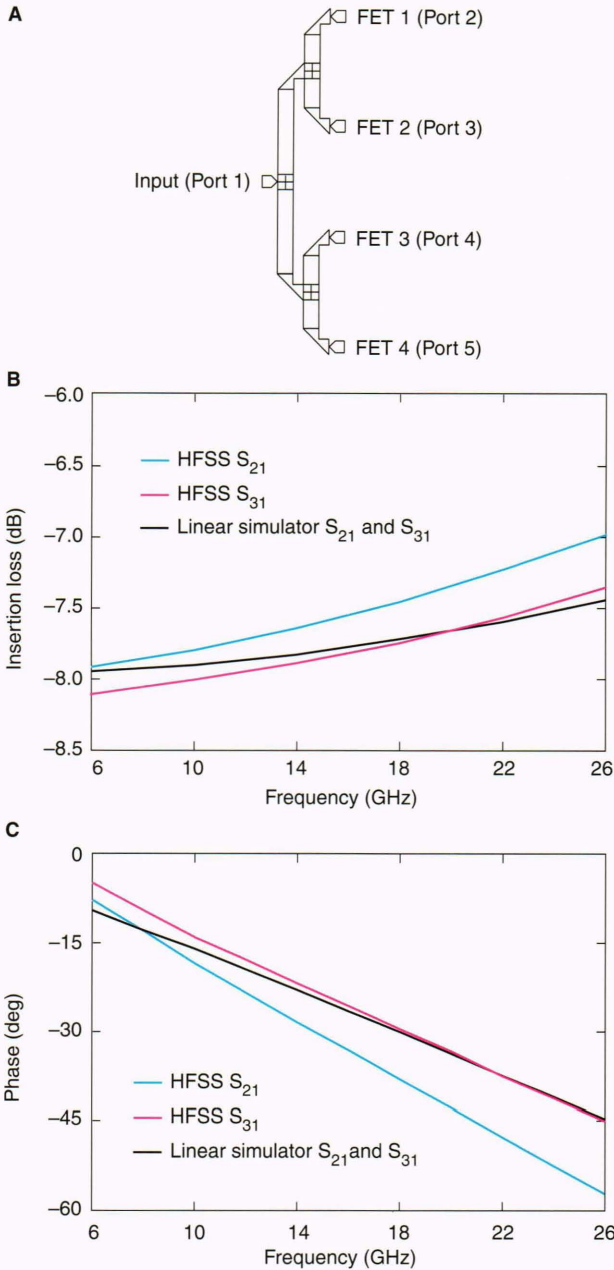
Figure 11. Power amplifier feed for four parallel field-effect transistors (FET's). **A.** Layout. **B.** S_{21} and S_{31} amplitude comparison between high-frequency structure simulator (HFSS) results and linear simulator results. **C.** S_{21} and S_{31} phase comparison between HFSS results and linear simulator results.

A

B

C

Figure 12. Coaxial-probe-fed microstrip antenna analysis: **A.** High-frequency structure simulator (HFSS) model. **B.** Electric field plot (Mag E: magnitude of electric field [volts/meter]). **C.** Visual standing wave ratio (VSWR) for a three- and six-iteration solution versus classical theory.

scattering parameters derived from the HFSS analysis with three and six iterations are compared with the theoretical predictions in Figure 12C.

The use of a resistive boundary makes the microstrip antenna problem computationally intensive. In addition, structures having high-quality factor resonances, such as microstrip antennas, are particularly troublesome for this type of simulator. It takes a number of convergences over a range of frequencies to "home in" on the resonance. The six-iteration solution for the 31.5-GHz antenna analysis was done on a 75-MIP machine with 128 Mbyte of RAM

running for several days. This problem represents the current limit of complexity that the software can handle on the most powerful workstations available in 1992. It is anticipated that the HFSS will be used in the future to determine the input return loss for other antennas such as waveguide horns.
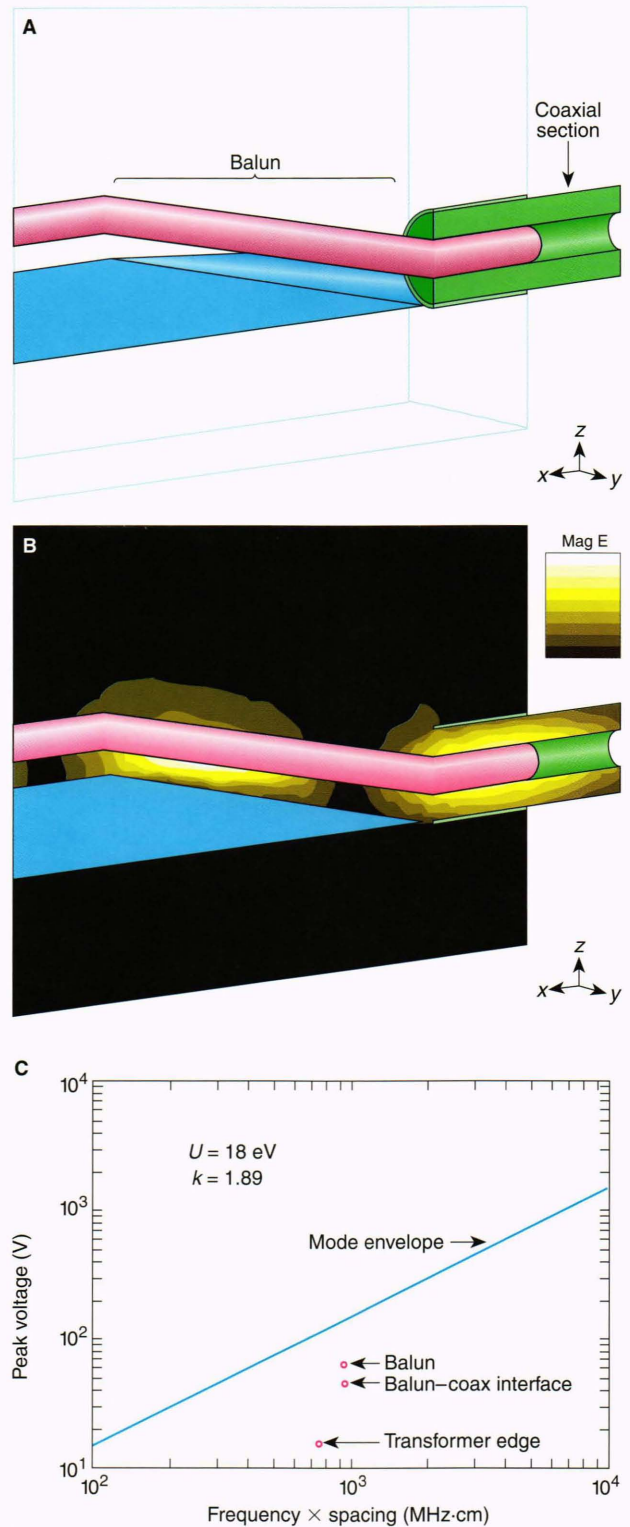
MULTIPACTOR BREAKDOWN ANALYSIS

Components in high-power microwave systems operating in a space environment may be subject to multipactor breakdown, which is an electron resonance discharge phenomenon that occurs only in a vacuum.[4] Multipactor breakdown can adversely affect the performance of components by causing excessive noise, resonant cavity detuning, erosion of component surfaces, and failure. In the past, approximate analytical techniques were used to predict the possibility of multipactor breakdown in components having simple geometries; for components having more complicated geometries, expensive and often unreliable testing was required. Past analytical techniques and tests can now be replaced by a numerical electromagnetic field solver that can provide an exact analysis of the electric fields inside the components. Once the magnitude of the fields is known, the potential for multipactor breakdown can be determined by comparing the field strength data with a plot of the multipactor existence region of the component.

Microwave design engineers at APL have performed a multipactor breakdown analysis of the Midcourse Space Experiment X-band antenna feed (Fig. 13) using the HFSS.[5] The HFSS model (Fig. 14A) showing the portion of the feed relevant to the analysis consists of an input coaxial section followed by a half-wave coax to two-wire (unequal diameters) balun. Figure 14B shows an electric field plot for this structure. The calculated voltages at
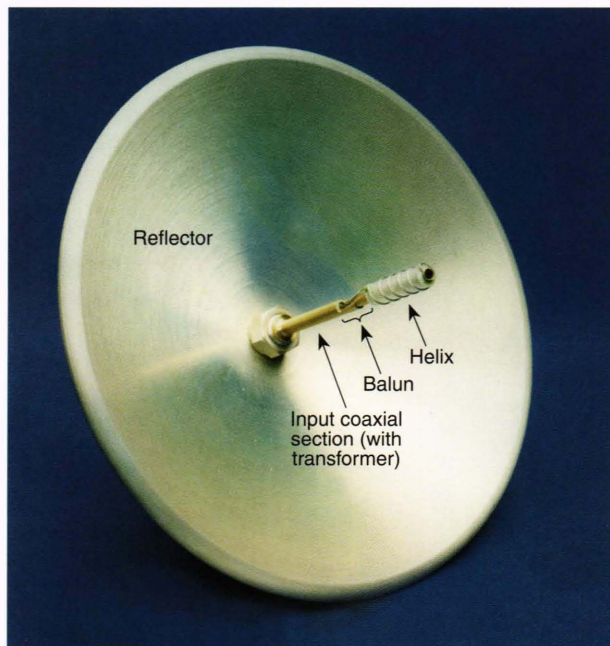
Figure 13. Midcourse Space Experiment X-band antenna.

Figure 14. Multipactor breakdown analysis for the Midcourse Space Experiment X-band antenna feed. **A.** High-frequency structure simulator (HFSS) model. **B.** Electric field plot (Mag E: magnitude of electric field [volts/meter]). **C.** Calculated voltages and multipactor breakdown existence region. Voltages falling above the mode envelope indicate possible multipactor breakdown problems. Voltages falling below the mode envelope indicate that no multipactor breakdown can occur. The voltages calculated for three sections in the antenna feed indicate that no multipactor breakdown can occur in the feed. U = electron kinetic energy. k = constant (determined by minimum kinetic energy required for secondary electron emission).

various points on the feed are plotted with the multipactor breakdown existence region plot in Figure 14C. Since the voltages in the feed fall below the multipactor breakdown existence region, multipactor breakdown cannot occur in this feed structure. This analysis eliminated the need for expensive environmental testing.

CONCLUSION

Microwave engineers at APL have successfully used a numerical electromagnetic field solver (the Hewlett–Packard HFSS) to accurately model microwave components such as transitions, waveguide components, MMIC components, and antennas. The field solver is a new modeling tool that will contribute significantly to the efficient, cost-effective design of present and future microwave systems.

REFERENCES

[1] Anger, A., "Software Computes Maxwell's Equations," *Microwave J.* **33(2)**, 170-178 (2 Feb 1990).
[2] Bialkowski, M. E., "Analysis of an N-Port Consisting of a Radial Cavity and E-Plane Coupled Rectangular Waveguides," *IEEE Trans. Microwave Theory Tech.* **40(a)**, 1840-1843 (Sep 1992).
[3] Penn, J. E., and Moore, C. R., "Model Verification of Passive MMIC Structures Through Measurement and 3D Finite Element Simulation," in *Proc. 3rd Annual Johns Hopkins Univ. Microwave Symp.*, Baltimore, Md., pp. I1-I13 (1992).
[4] Clancy, P. F. "Multipactor Control in Microwave Space Systems," *Microwave J.* **30**, 77-83 (Mar 1978).
[5] Jablon, A. R., "Spacecraft Antenna Multipactor Analysis Using a Numerical Electromagnetic Simulator," in *Proc. 3rd Annual Johns Hopkins Univ. Microwave Symp.*, Baltimore, Md., pp. IX1-IX12 (1992).

THE AUTHORS
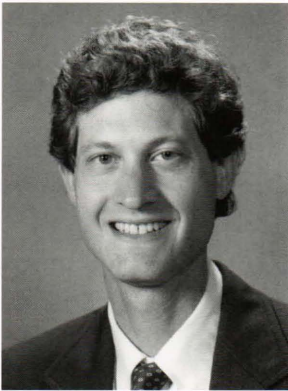
ALLAN R. JABLON is a member of the APL Senior Staff and is an engineer in the Microwave and RF Systems Group in the Space Department. He received an M.S. in electrical engineering from The Johns Hopkins University G.W.C. Whiting School of Engineering in 1990 and a B.S.E.E. from Virginia Polytechnic Institute and State University in 1986. Since joining APL in 1986, he has worked in antenna design, development, and testing as well as in RF systems, and microwave circuit design. He has designed and developed antennas for the TOPEX, SALT, and MSX spacecraft programs.

CRAIG R. MOORE is a member of APL's Principal Staff. He received B.E.E. and M.S. degrees from Cornell University in 1962 and 1964, respectively. He previously served as associate division head at the National Radio Astronomy Observatory, principal research associate for the Australian government, and group manager at Bendix Field Engineering Corporation, before joining APL in 1987. His work at the Laboratory has involved improvements to the hydrogen maser, work on ultra-high-Q cryogenic microwave resonators, and MMIC design and testing. He is currently project manager for an ultra-small satellite terminal design effort. Mr. Moore is a senior member of the IEEE and has authored more than twenty papers. He teaches MMIC design at The Johns Hopkins University G.W.C. Whiting School of Engineering.
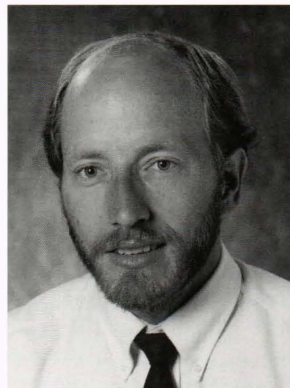
JOHN E. PENN is a member of APL's Senior Staff. He received a B.E.E. from The Georgia Institute of Technology in 1980, and M.S. degrees in electrical engineering and computer science from The Johns Hopkins University in 1982 and 1988, respectively. Mr. Penn joined APL in 1980, where his work has involved custom integrated circuit design, semi-custom design, silicon compiler design, digital design, programming, and, more recently, microwave design. He left the Laboratory in 1990 to work as an applications engineer for Silicon Compiler Systems, which became part of Mentor Graphics. In 1992, he rejoined the Laboratory in the S2R Group where he has been designing MMIC's. Mr. Penn co-teaches a MMIC design course with Craig Moore at The Johns Hopkins University G.W.C. Whiting School of Engineering.